CHAPTER IV

ANIONIC SURFACTANT AIDED PREPARATION OF HIGH SURFACE AREA AND HIGH THERMAL STABILITY CERIA-ZIRCONIA MIXED OXIDE FROM CERIUM AND ZIRCONIUM GLYCOLATES VIA SOL-GEL PROCESS AND ITS REDUCTION PROPERTY

(Applied Organometallic Chemistry, 22 (2008) 167-170)

4.1 Abstract

This work was focused on the ceria zirconia mixed oxide prepared through a surfactant-introduced synthesis method. High surface area nanoparticle mesoporous ceria zirconia mixed oxide was successfully synthesized. The surface features, textural properties, and crystalline structure of the ceria zirconia mixed oxides were studied by means of thermogravimetric analysis (TGA), N_2 physisorption isotherms, fourier transform infrared spectroscopy (FT-IR), scanning electron micrographs (SEM), and X-ray diffraction (XRD) techniques. High surface area, mesoporous fluorite-structured CeO_2-ZrO_2 was obtained from the elimination of surfactants upon calcination process. A surface area in excess of 205.6 m^2/g was obtained after calcination at 500°C, and dropped to 75.96 m^2/g by heating at 900°C. TPR results showed that the lowest reduction temperature was obtained from the sample containing 40% zirconia content.

Keywords: Ceria, Zirconia, Sol-gel process, TPR and Anionic surfactant

4.2 Introduction

Ceria-based materials are widely used in automotive pollution control[1]. Ceria is known to be an excellent oxygen buffer; however, it still requires enhancement of its thermal stability. Recent studies report the improvement of textural properties by introducing doping elements in the CeO_2 fluorite-type lattice, and the most efficient dopant studied was zirconium, as excellently discussed by our previous work[2]. Due to their use in the TWCs, the thermal stability required for CeO_2-based oxides has changed over the years as the converter technology continued its development[3, 4]. Nowadays, thermal stability up to 1373 K is typically required for the catalysts closely coupled to the engine, which requires an extremely robust design of the textural properties of the material

This success depends on the molecular homogeneity, surface area and textural/morphological properties, which are affected by the appropriate selection of precursor, preparation methods and the mixing composition[2]. There are many different synthesis methods that have been applied to prepare CeO_2-ZrO_2 and related mixed oxides, including co-precipitation[5, 6] high energy ball-milling[7], and sol-gel[8]. The sol-gel process is a versatile technique, allowing control of the texture, composition, homogeneity, and structural properties of solids[9]. Generally, Ce-rich compositions are preferred for catalysis purposes and the best results are obtained using $Ce_xZr_{1-x}O_2$ with x ranging from 0.6 to 0.8[10]. The surface areas of ceria-zirconia obtained by either conventional co-precipitation or sol-gel were typically in the range of 60-90 m^2/g after calcination with air at 700-800 K[11, 12].

The use of a templating technique for the synthesis of mesoporous solids has recently opened up new opportunities in the design of novel high surface area materials for catalytic applications. Much interest is being focused on the preparation of transition metal oxides using several templating pathways[13-15]. Several meso-structured surfactant-oxide composites have been synthesized by this approach, and a few of these composites showed a regular pore structure even after calcination[16, 17] while the majority suffered

from collapse of the regular pore structure after calcination[18]. Zirconia is currently under extensive investigation in this area and several different approaches have been developed using cationic[19, 20], anionic[21] or amphoteric routes[22] to expand the range of surface areas available. There are some reports using cationic surfactant as a template for ceria zirconia mixed oxide preparation[23, 24], but no reports describe the use of an anionic surfactant as a template in these mixed oxide preparations, especially by the sol gel method. The objective of this present study was thus to improve textural, structural, and chemical properties of ceria-based catalyst for environmental application using an anionic surfactant template via the sol-gel route at ambient temperature. A study on its reduction property was also investigated.

4.3 Methodology

4.3.1 Mixed oxide preparation

Mixed oxide catalysts were prepared via the sol-gel process using cerium glycolate and sodium tris(glycozirconate) precursors synthesized via the Oxide One Pot Synthesis (OOPS) process[25]. The starting glycolate materials were mixed with 1 M sodium hydroxide and aqueous sodium dodecyl sulfate (SDS) at 1:2:1 mole ratio. The ratio between each metal alkoxide was varied, depending on desired compositions: $Ce_xZr_{1-x}O_2$, where x = 0.2-0.8. The mixture was stirred for 2 h to obtain a gel and was further kept at room temperature for 2 and 10 days to study the significant effect of aging time on the degree of incorporation of the surfactant and the solid solution since less than 2 days aging time provided no gelation while aging times between 3-9 days gave non homogeneous results. After the aging step, the gels were washed with deionized water three times to remove the Na content generated from sodium tris(glycozirconate), free surfactant and NaOH added during gelation step. The samples were then put in an oven at 110°C for at least 12 h to let them dry before calcination at 500° or 900°C for 2 h in air. It should be noted here that samples calcined at 700°C show the same structure and morphology as those calcined at 500°C, which is in good

agreement with our previous work[2].

The homogeneity was investigated by calcining samples at 1000°C for 5 h because this condition is critical since lower calcination temperatures do not allow fine non-homogeneities to be revealed[26].

4.3.2 Characterization

The structure of the samples was determined from a wide-angle X-ray diffractometer (WXRD), a Rigaku D/MAX 2000, using CuK$\propto$ radiation (λ = 1.5406 Å). The intensity data were collected at 25°C over 2θ range of 5-90°. Peak positions were compared with standard JCPDS files to identify the crystalline phases. The average grain size (D) was estimated according to the Scherrer equation:

$$D = 0.94\lambda / \beta \cos\theta$$

where θ is the diffraction angle of the (111) peak of the cubic phase or the (101) peak of the tetragonal phase and β is the full width at half-maximum (fwhm) of the (111) or the (101) peak (in radian)[2]. Lattice parameters of samples are calculated by using Vegard rule:

$$a_{average} = (2(2\sqrt{2}a)+c)/3$$

The cell parameter a is considered in the case of the cubic symmetry.

Scanning electron micrographs (SEM) were obtained on a JOEL 5200-2AE (MP15152001). Surface areas and pore size of all powder samples were determined by N_2 adsorption at 77 K using a Quantachrome Corporation Autosorb. Fourier transform infrared (FT-IR) spectra were recorded on a VECTOR 3.0 BRUKER spectrophotometer with a spectral resolution of 4 cm^{-1} to examine the functional groups of the synthesized precursor. The solid sample was obtained using a transparent KBr pellet containing 1% sample mixed with 99% dried KBr. Thermal behavior and stability

of the as-synthesized ceria-zirconia mixed oxides were investigated using thermogravimetric/differential thermal analyses (TGA/DTG) on a Perkin-Elmer Pyris Diamond TG/DTA. A ramp rate of 10°C/min was used under oxygen. A Micromeritics TPD/TPR 2900 was employed as an analyzer for the temperatures of the thermal conductivity detector, using a furnace temperature up to 900°C at a linear ramp rate of 10°C/min, and 5% hydrogen in nitrogen used as the carrier gas with a flow rate of 50 ml/min. The sample was pretreated by flowing He over the sample at 120°C for 4h before analysis.

4.4 Results and Discussion

The homogeneity of solid solutions is dependent on reaction times, being lower for reaction times of less than 2 days. This is probably due to an incomplete exchange reaction between the hydroxyl groups of the hydrous oxide and the surfactant[23]. When these solids are dried, the capillary pressure at the liquid-vapor interface in the pores produces stress on the metal oxide framework, thus provoking the collapse of the pore network and, in turn, reducing their surface area. In the case when the surfactant is present, the capillary pressure in the pores is generally proportional to the surface tension because the surfactant can reduce water surface tension in the pores. This will reduce the shrinkage and collapse of the network during drying and calcination, which could help to maintain high surface areas and improve thermal stability of samples[23]. In addition, the mixed oxides show a good compositional homogeneity and thermal stability after aged for 10 days.

The average particle sizes calculated by the Scherrer equation for $Ce_xZr_{1-x}O_2$ powders are listed in Table 4.1. The average particle sizes of mixed oxides are increase with the doping of CeO_2. The particle sizes of oxides are increase after calcinations at higher temperature due to the sintering process but decrease as the aging times increase because oxides, which have longer aging time, are more difficult to sinter. However, the pure oxides are sintered the easiest especially CeO_2.

The average lattice parameter "a" is considered in the case of cubic symmetry[23, 26]. The six main reflections typical of fluorite-like structured material with a fcc cell, corresponding to the {111}, {200}, {220}, {311}, {222}, and {400} planes. Values of a in the range of 0.52-0.54 nm were obtained from mixed oxide catalysts. These results are in agreement with those obtained from Ce-Zr-O prepared by other routes and are consistent with calculations made from empirical relationships[2, 23].

N_2 adsorption/desorption studies were carried out on samples calcined at different temperatures in order to investigate the effect of calcinations temperature on surface area and porosity, which can refer to the thermal stability of the catalysts.

The data are summarized in Table 4.1. The minimum calcinations temperature was 500°C. At this temperature, all the organic residues were removed and detected using TGA (not shown).

BET surface areas of the mixed oxides calcined at 500° and 900°C are higher than those of pure oxides and decrease as the crystallite size increases after calcining at higher temperature.

Figure 4.1 shows the thermal stability of mixed oxides. It increased when increasing the amount of zirconia up to 40%. This can be explained by the following: the addition or incorporation of zirconia to ceria as mixed oxides can enhance the thermal stability of CeO_2, resulting in better resistance of the sintering and deactivation processes. It is clear that CeO_2 undergoes a rapid crystallite growth process since BET surface areas of both catalysts using the aging times of 2 and 10 days decrease significantly more than those of mixed oxide samples. Therefore, the crystallite growth process is retarded by the incorporation of Zr ion into the CeO_2 matrix[2]. The results also showed that when increasing aging time, the higher surface area obtained and thermal stability also increases. This is probably due to the complete exchange reaction between the hydroxyl groups of the hydrous oxide and the surfactant in the samples after aging for 10 days. These results also indicate that the surfactant aided preparation yields ceria zirconia mixed oxide of higher surface area and higher thermal stability than those reported by many researchers[23-24, 28-32].

The highest surface area and thermal stability obtained from $Ce_{0.6}Zr_{0.4}O_2$ aged for 10 days. Its N_2 isotherms are type IV, indicating mesoporous structure but the loop change shape and average pore diameter increase from 3.614 to 6.126 nm after calcined at higher temperature (not shown) because of a reduction of mesopore fraction in the samples.

FT-IR spectra of $Ce_{0.6}Zr_{0.4}O_2$ aged for 10 days shown in Figure 4.2. The hydrocarbon deformation and stretching modes (1400-1500 cm^{-1}, 2800-3000 cm^{-1}) related to the surfactant incorporated in the solid[23] can be seen in as-synthesized sample. When the calcinations temperature was increased to 900°C, the bands at approximate 2800-2900 and 1600 cm^{-1} decrease significantly, showing that most of the surfactant and the adsorbed water were removed from the sample.

The other bands in the IR spectrum are due to the presence of residual OH from water adsorbed on the sample (3500 and 1600 cm^{-1}). However, because of the overlapping of the C-H bond and the hydroxyls absorption in this range, it is not possible to clearly distinguish.

The band at 550 cm^{-1} refers to Zr(Ce)-O stretching[1]. The results are in agreement with those obtained by Terribile *et al.*[23]. The other samples give similar FTIR spectra, even at different aging times (not shown).

The thermogravimetric profile of $Ce_{0.6}Zr_{0.4}O_2$ aged for 10 days shown in Figure 4.3. The first effect is attributed to the release of adsorbed water, the second to desorption and decomposition of the surfactant, and the third to dehydroxylation of the surface.

XRD spectra of samples calcined at 500° and 900°C are in Figures 4.4 and 4.5, respectively. Expectedly, the XRD peaks become sharper with increasing calcinations temperature, indicating an increase in the crystallite size and crystallization of the amorphous phase due to partial sintering[26].

The pure oxide peaks indicate cubic CeO_2 and tetragonal ZrO_2 after heating at 500°C for 2 h. Additional monoclinic phase ZrO_2 appears with the peaks at $2\theta = 28°$ and

31° after heating at 900°C for 2 h. In other words, the monoclinic phase is preferable at higher temperature, which is in good agreement with the results reported elsewhere[33, 34].

In the patterns of the oxides with intermediate composition, the reflections are broader, showing that the crystallite size is smaller. The reflections in these patterns systematically shift, due to shrinkage of the lattice, to lower *d*-spacing when cerium is replaced by zirconium. This shrinkage phenomenon coincides with the fact that the cation radius of Zr^{4+}(0.84 Å) is smaller than that of Ce^{4+}(0.97 Å)[26].

Single phase mixed oxides can be achieved in ceria rich region after aged for 10 days that have been characterized by calcinations at 1000°C for 5 h (Figure 4.6).

Compared to the mixed oxides aged for only 2 days and calcined at 900°C 2 h, those aged for 10 days give more homogeneous products. Unlike pure oxide, the aging time causes no effect on XRD results.

The reactivity of lattice oxygen in ceria zirconia mixed oxide catalysts towards H_2 was investigated by TPR technique (Figure 4.7). The two-peak pattern due to surface (low temperature peak), and bulk reduction (high temperature peak) clearly seen in CeO_2[35]. These 2 peaks are merged together in the solid solutions. This suggests that the whole ceria component, including bulk part, in the solid solutions is subjected to reduction in a single stage. The single stage reduction of solid solutions can be explained in terms of facile migration of oxygen ions in the CeO_2-ZrO_2 lattice[36]. The variation in temperature profile seems to be related to the ZrO_2 content in the sample and may have some structure dependency as well[37]. The H_2 consumption of the mixed oxide is higher than that of the CeO_2 alone. This means that the presence of ZrO_2 improves the reduction property of CeO_2. The reduction of the bulk lattice oxygen in the solid solution becomes easier because of the distortion of the structure, which is caused by the partial substitution of Ce^{4+} with Zr^{4+} in the sol-gel technique. As a result, reduction of the bulk lattice oxygen must occur simultaneously with the reduction of surface oxygen. This occurs through structural modifications of the fluorite-type lattice of ceria as a consequence of the substitution of Ce^{4+} (ionic radius 0.97 Å) with Zr^{4+} (ionic radius 0.84 Å). The effect of this substitution is to decrease cell volume, lowering the activation

energy for oxygen-ion diffusion within the lattice, and consequently favoring reduction. The introduction of zirconium also enhances the formation of structural defects, which are expected to play an important role in determining reduction/oxidation behavior. This result is in agreement with many previous works[33, 38]. In contrast with the pure CeO_2 and mixed oxides, only a very small amount of H_2 was consumed for ZrO_2 because ZrO_2 does not get reduced below 1000 K[35].

It clearly appears from the TPR results that mixed oxides show better reducible properties than many researches[39-41] and the lowest reduction temperatures are observed in $Ce_{0.6}Zr_{0.4}O_2$. The redox behavior of ceria based mixed oxides is important feature because most catalysts used for the oxidation reaction are under the redox cycle.

The SEM images of $Ce_{0.6}Zr_{0.4}O_2$ aged for 10 days (Figure 4.8) show effect of heat treatments on morphology (magnification = 7500x). The picture shows particle aggregates of sphere shapes and small sizes before calcining. After calcining at 500° and 900°C the particles become irregular shaped and larger sized due to the collapse in structure after heat treatment. The aging time has no effect in morphology for compositions: $Ce_xZr_{1-x}O_2$, as investigated by SEM (not shown).

4.5 Conclusions

The influences of various synthesis parameters are investigated. The sample using Ce:Zr equal to 6:4 and aged for 10 days gives the highest surface area (205.6 m^2/g). Aging time causes significant effect to textural and structure of mixed oxides. Calcinations of the mixed oxide gels at 500° and 900°C crystallizes the mixed oxide domains and strongly affects the porosity and surface areas for these pore-solid nanoarchitectures. Heat treatment reduces the void volume, changes the pore-size distribution, and increases the average grain size. The mixed oxides show a good compositional homogeneity and thermal stability, which is an important requirement in these materials for applications in the formulation of catalysts for auto-exhaust treatment.

4.6 Acknowledgments

The authors gratefully acknowledge the financial support of the Postgraduate Education and Research Program in Petroleum and Petrochemical Technology Thailand, the PPT Consortium (ADB) Fund Thailand and the Ratchadapisake Sompote Fund, Chulalongkorn University.

4.7 References

1. Trovarelli C, Leitenburg M, Boaro G. *Catal. Today* 1999; 50: 353.
2. Rumruangwong M, Wongkasemjit S. *Appl. Organometal. Chem.* 2006; 20: 615.
3. Shelef M, McCabe RW. *Catal. Today* 2000; 62: 35.
4. Heck RM, Farrauto RJ. *Appl. Catal. A* 2001; 221: 443.
5. Leitenburg C, Trovarelli A, Bini G, Cavani F, Llorca J. *Appl. Catal. A: General* 1996; 139: 161.
6. Hori CE, Permana H, Ng KYS, Brenner A, More K, Rahmoeller KM, Belton D. *Appl. Catal. B* 1998; 16: 105.
7. Trovarelli A, Zamar F, Llorca J, Leitenburg C, Dolcetti G. Kiss J. *J. Catal.* 1997; 169: 490.
8. Fornasiero P, Balducci G, Monte RD, Kas˘par J, Sergo V, Gubitosa G, Ferrero A, Graziani M. *J. Catal.* 1996; 164: 173.
9. Cauqui MA, Rodriguez-Izquierdo Rodriguez-Izquierdo JM. *J. Non-Cryst. Solids* 1992; 147/148: 724.
10. Trovarelli A. *Catal. Rev.- Sci. Eng.* 1996; 38: 439.
11. Fornasiero P, Balducci G, Monte RD, Kas˘par J, Sergo V, Gubitosa G, Ferrero A, Graziani M. *J. Catal.* 1996; 164: 173.
12. Leitenburg C, Trovarelli A, Bini G, Cavani F, Llorca J. *Appl. Catal. A: General* 1996; 139: 161.
13. Kresge CT, Leonowicz ME, Roth WJ, Vartuli JC, Beck JS. *Nature* 1992; 359: 710.

14. Huo Q, Margolese DI, Ciesla U, Feng P, Gier TE, Sieger P, Leon R, Petroff PM, SchuÈ th B, Stucky GD. *Nature* 1994; 368: 317.
15. Tanev PT, Pinnavaia TJ. *Science* 1995; 267: 865.
16. Ciesla U, Schacht S, Stucky GD, Unger KK, SchuÈ th F, Angew. *Chem. Int. Ed. Engl.* 1996; 35: 541.
17. Antonelli DM, Ying JY, Angew. *Chem. Int. Ed. Engl.* 1996; 35: 426.
18. Huo Q, Margolese DI, Ciesla U, Demuth DG, Feng P, Gier TE, Sieger P, Firouzi A, Chmelka BF, SchuÈ th B, Stucky GD. *Chem. Mater.* 1994; 6: 1176.
19. Hudson MJ, Knowles JA. *J. Mater. Chem.* 1996; 6: 89.
20. Reddy JS, Sayari A. *Catal. Lett.* 1996; 38: 219.
21. Larsen G, Lotero E, Nabity M, Petkovic LM, Shobe DS. *J. Catal.* 1996; 164: 246.
22. Kim A, Bruinsma P, Chen Y, Wang LQ, Lin J. *Chem. Commun.* 1997; 161.
23. Terribile D, Trovarelli A, Liorca J, Leitenburg C, Dolcetti G. *Catal. Today* 1998; 43: 79.
24. Chen LF, González G, Wang JA, Noreña LE, Toledo A, Castillo S, Morán-Pineda M. App. Surf. Sci. 2005; 243: 319.
25. Ksapabutr B, Gulari E., Wongkasemjit S. *Mater. Chem. and Phy.* 2004; 83: 34.
26. Monte RD, Kasˇpar J. *J. Mater. Chem.* 2005; 15: 633.
27. Sun Y, Sermon PA. *J. Mater. Chem.* 1996; 6: 1025.
28. Chen W, Li F, Yu J, Liu L, Gao H, *Mater. Res. Bull.* 2006; 41:2318.
29. Huber F, a Venvik H, Rønning M, Walmsley J, Holmena A, *Chem. Eng. J* article in press.
30. Rui S, Ya-Wen Z, Shi-Jie L, Bing-Xiong L, Chun-Hua Y. *J. Phys. Chem. B* 2004; 108: 12481.
31. Daturi M, Finocchio E, Binet C, Lavalley CJ, Fally F, Perrichon V, Vidal H, Hickey N, Kasˇpar J. *J. Phys. Chem. B* 2000; 104: 9186.
32. Kim T, Vohs JM, Gorte RJ. *Ind. Eng. Chem. Res.* 2006; 45: 5561.
33. Kasˇpar J, Fornasiero P, Graziani M, Trovarelli A. *J. Catal.* 1995; 151: 168.

34. Kasˇpar J, Vidal H., Daturi M., Finocchio E., Binet C. *J. Phys. Chem. B* 2000; 104: 9186.

35. Ranga Rao G. *Bull. Mater. Sci.* 1999; 22: 89.

36. Murata T, Hasegawa T, Aozasa S, Matsui H, Motoyama M. *J. Alloys and comp.* 1993; 193: 298.

37. Ranga Rao G, Fornasiero P, Kasˇpar J, Mariani S, Di Monte R, Graziani M. *Stud. Surf. Sci. Catal.* 1995; 96: 631.

38. Kasˇpar J, Vidal H, Daturi M, Finocchio E, Binet C. *J. Phys. Chem. B* 2000; 104: 9186.

39. Yeste MP, Herna´ndez JC, Bernal S, Blanco G, Calvino JJ, Jose´ A. Omil P, Pintado JM. *Chem. Mater.* 2006; 18: 2750.

40. Guo Y, Lu G, Zhang Z, Zhang S, Qi Y, Liu Y. *Catal. Today* 2007; 126: 296.

41. Ozaki T, Masui T, Machida K, Adachi G, Sakata T, Mori H. *Chem. Mater.* 2000; 12: 643.

Table 4.1 Physical properties of ceria zirconia mixed oxide as a function of heat treatment

Ce : Zr	Aging time (day)	Calcinations temperature (°C)	Average particle size XRD (nm)	Surface area (m^2/g)
ZrO_2	2	500	9.03	80.00
		900	17.08	20.12
2:8		500	5.19	98.06
		900	11.65	28.44
4:6		500	6.85	99.87
		900	12.09	32.68
6:4		500	7.93	107.65
		900	13.12	35.76
8:2		500	8.15	105.12
		900	14.23	28.85
CeO_2		500	10.05	92.35
		900	18.96	20.13
ZrO_2	10	500	9.02	100.65
		900	17.42	30.05
2:8		500	4.94	110.22
		900	10.96	37.26
4:6		500	6.06	120.47
		900	11.83	42.9
6:4		500	7.12	205.6
		900	12.95	75.96
8:2		500	8.02	192.17
		900	14.01	62.23
CeO_2		500	9.21	105.14
		900	18.14	23.44

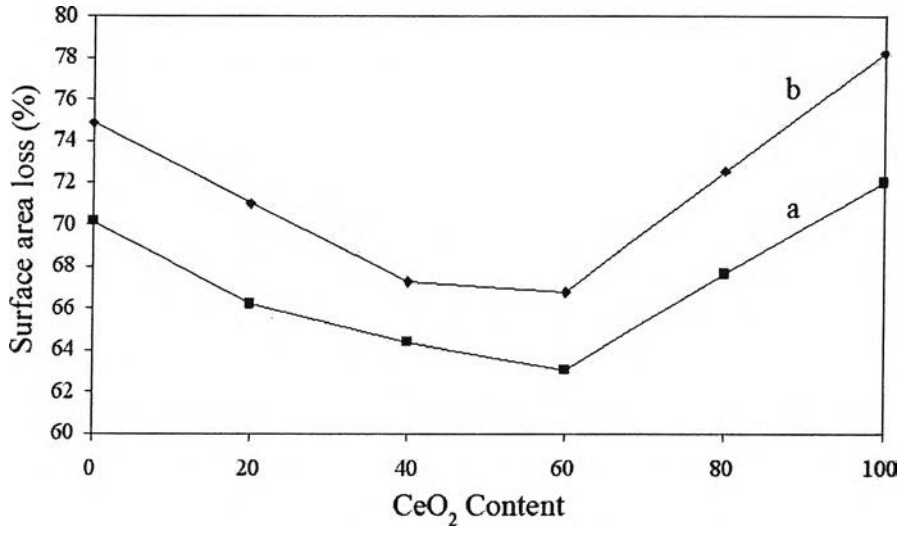

Figure 4.1 Loss of surface areas due to calcinations (from 500° to 900°C) for ceria-zirconia mixed oxides with various aging time: (a) 10 days; (b) 2 days.

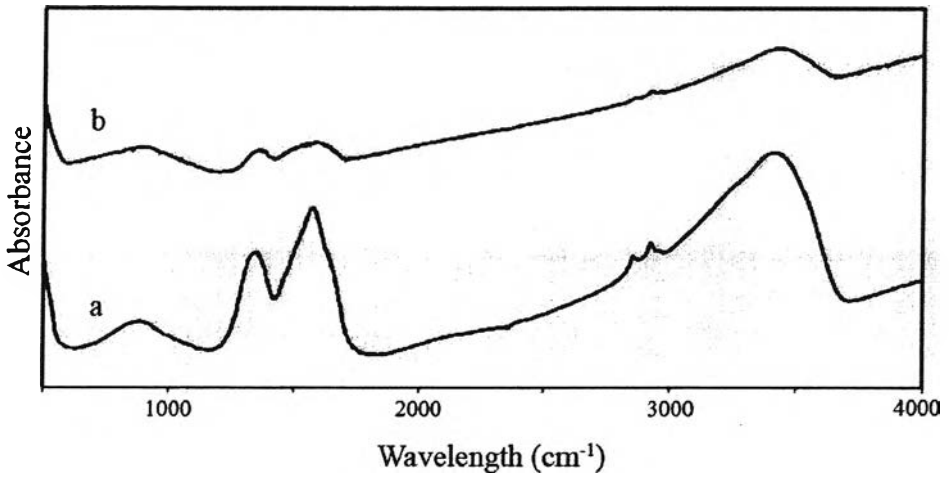

Figure 4.2 FTIR spectra of $Ce_{0.6}Zr_{0.4}O_2$ aged for 10 days: (a) dried at 110°C/24 h; (b) calcined at 500°C/2 h under.

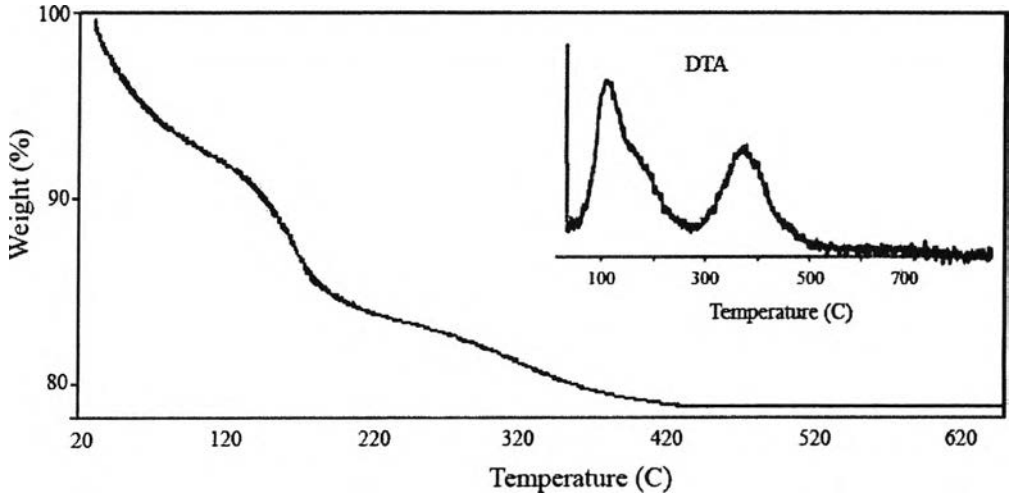

Figure 4.3 TGA profile of as-synthesized $Ce_{0.6}Zr_{0.4}O_2$ aged 10 days. The insert display shows corresponding DTA curve.

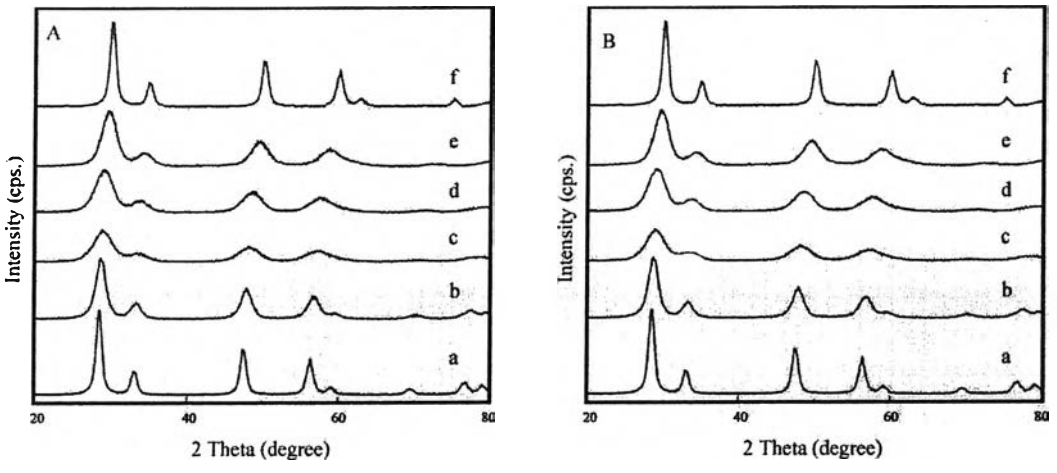

Figure 4.4 XRD patterns for ceria-zirconia mixed oxides aged for (A) 2 days and (B) 10 days calcined at 500°C/2 h: (a) CeO_2; (b) $Ce_{0.8}Zr_{0.2}O_2$; (c) $Ce_{0.6}Zr_{0.4}O_2$; (d) $Ce_{0.4}Zr_{0.6}O_2$; (e) $Ce_{0.2}Zr_{0.8}O_2$; (f) ZrO_2.

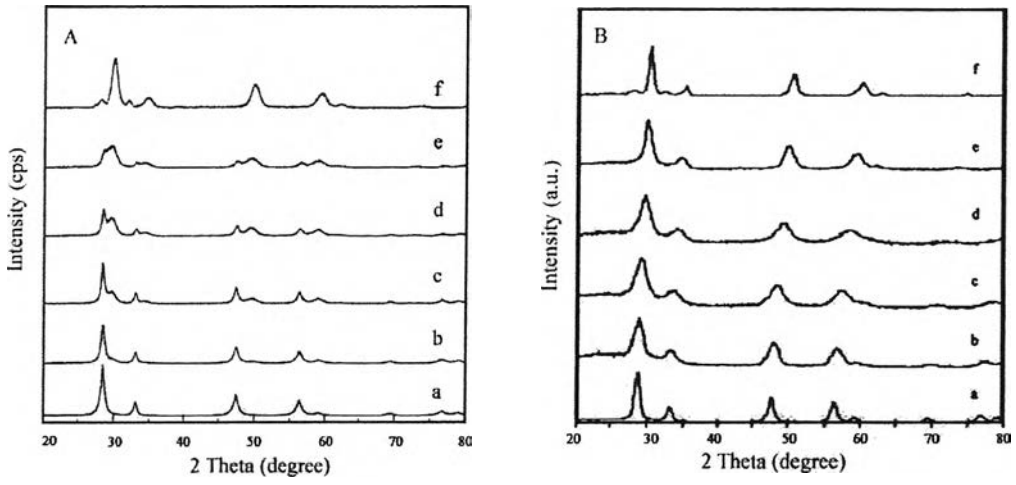

Figure 4.5 XRD patterns for ceria-zirconia mixed oxides aged for (A) 2 days and (B) 10 days calcined at 900°C/2 h: (a) CeO_2; (b) $Ce_{0.8}Zr_{0.2}O_2$; (c) $Ce_{0.6}Zr_{0.4}O_2$; (d) $Ce_{0.4}Zr_{0.6}O_2$; (e) $Ce_{0.2}Zr_{0.8}O_2$; (f) ZrO_2.

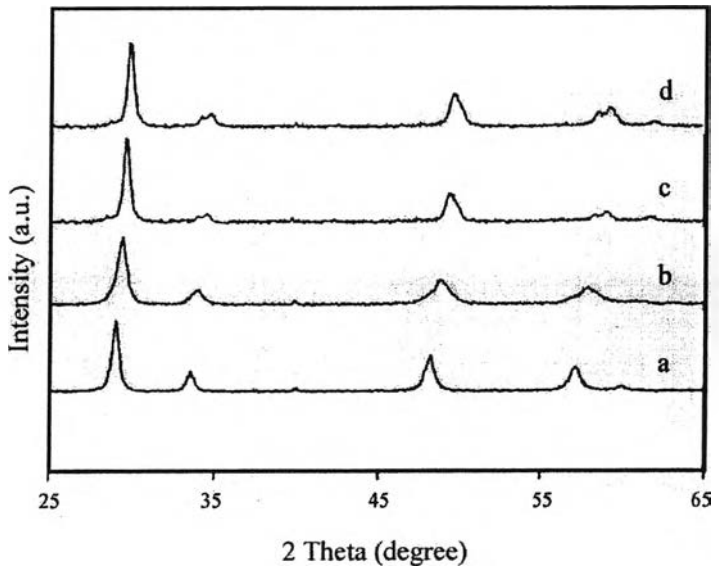

Figure 4.6 XRD patterns for ceria-zirconia mixed oxides aged for 10 days calcined at 1,000°C/5 h: (a) $Ce_{0.8}Zr_{0.2}O_2$; (b) $Ce_{0.6}Zr_{0.4}O_2$; (c) $Ce_{0.4}Zr_{0.6}O_2$; (d) $Ce_{0.2}Zr_{0.8}O_2$.

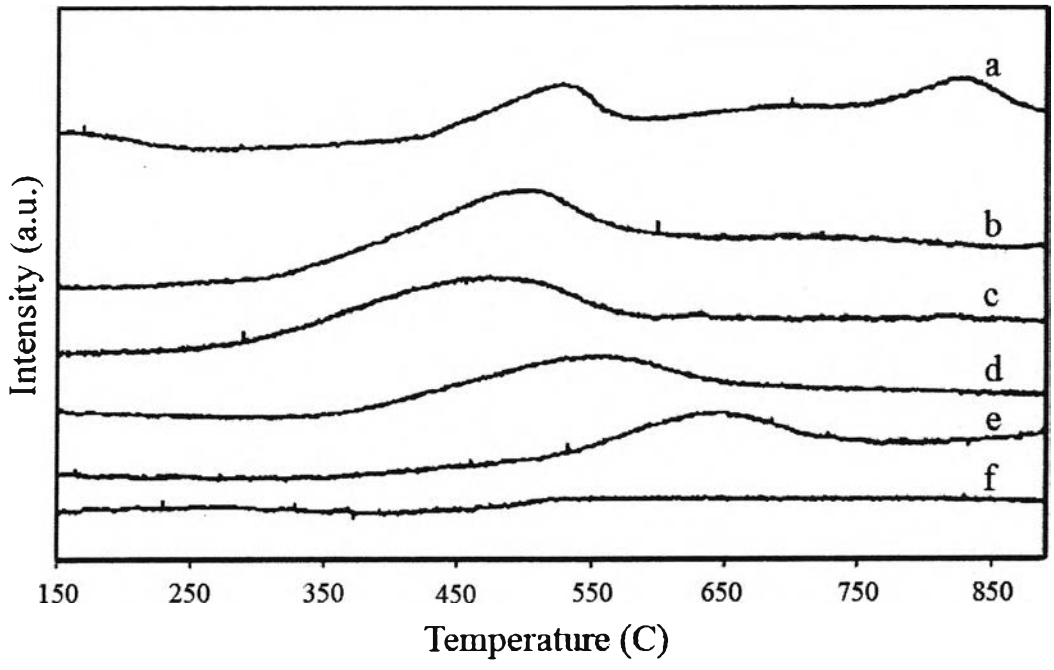

Figure 4.7 TPR profiles of ceria-zirconia mixed oxides aged for 10 days and calcined at 500°C/ 2 h: (a) CeO_2; (b) $Ce_{0.8}Zr_{0.2}O_2$; (c) $Ce_{0.6}Zr_{0.4}O_2$; (d) $Ce_{0.4}Zr_{0.6}O_2$; (e) $Ce_{0.2}Zr_{0.8}O_2$; (f) ZrO_2.

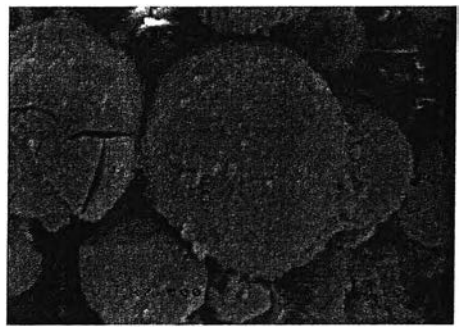

a

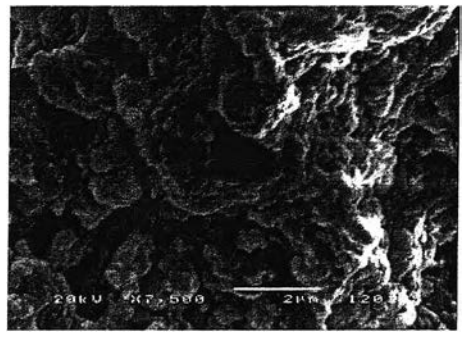

b

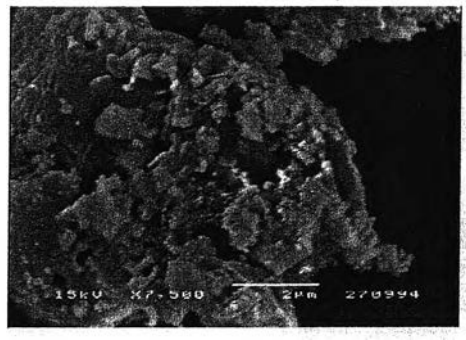

c

Figure 4.8 SEM micrographs of $Ce_{0.6}Zr_{0.4}O_2$ aged 10 days (a) as-synthesized; (b) heated at 500°C/ 2 h; (c) heated at 900°C/ 2 h.